

# Journal of Advanced Pharmacy Research

## Section C: Drug Design, Delivery & Targeting



### Investigation and Physicochemical Characterization of Binary Febuxostat-Sulfobutyl Ether $\beta$ -Cyclodextrin Inclusion Complexes

Wedad Sakran, Rania S. Abdel-Rashid\*, Mai Abdel-Hakim, Mohamed Teiama

Pharmaceutics and Industrial Pharmacy Department, Faculty of Pharmacy, Helwan University,  
Ain Helwan, Cairo 11795, Egypt

\*Corresponding author: Rania S. Abdel-Rashid, Pharmaceutics and Industrial Pharmacy Department, Faculty of Pharmacy, Helwan University, Ain Helwan, Cairo 11795, Egypt. Tel. (+2)01156995596  
Email address: [rania.safa@pharm.helwan.edu.eg](mailto:rania.safa@pharm.helwan.edu.eg)

Submitted on: 11-06-2022; Revised on: 26-06-2022; Accepted on: 28-06-2022

To cite this article: Sakran, W.; Abdel-Rashid, R. S.; Abdel-Hakim, M.; Teiama, M. Investigation and Physicochemical Characterization of Binary Febuxostat- Sulfobutyl Ether  $\beta$ -Cyclodextrin Inclusion Complexes. *J. Adv. Pharm. Res.* **2022**, 6 (3), 133-143. DOI: [10.21608/aprh.2022.144204.1178](https://doi.org/10.21608/aprh.2022.144204.1178)

#### ABSTRACT

**Background:** Febuxostat (FBX) a non-purine, xanthine oxidase inhibitor that is commonly indicated for the treatment of chronic gout. Yet, it is suffering from limited application as it belongs to The BCS II class that exhibit poor solubility. The aim of this study was to explore the impact of complexation between Febuxostat (FBX) and Sulfobutylether beta-cyclodextrin (SBE- $\beta$ -CD) on physicochemical properties of FBX and its dissolution behavior. **Methods:** Different batches of inclusion complexes were formulated using various drug to polymer ratios (1:1, 1:3, and 1:5). The complexes were formulated with SBE- $\beta$ -CD via four different techniques (physical mixture, kneading method, solvent evaporation and freeze drying). The inclusion complexes were examined by Fourier transformation infrared spectroscopy (FTIR), Scanning electron microscopy (SEM), Differential scanning calorimetry (DSC), and Particle size analysis. The dissolution of different formulated FBX complexes was also studied. **Results:** The FTIR and DSC results suggested that FBX was incorporated inside the core of SBE- $\beta$ -CD to give inclusion complexes. In comparison to the other techniques, inclusion complex produced by freeze drying using SBE- $\beta$ -CD (1:5 ratio of drug to polymer) produced significantly higher Inclusion Efficiency (IE %). Moreover, the FBX- SBE- $\beta$ -CD inclusion complex displayed higher aqueous solubility compared with free FBX, suggesting its potential application in pharmaceutical formulations. **Conclusion:** Freeze drying technique had successfully formed a binary system complex between FBX and SBE- $\beta$ -CD with better dissolution behavior. For further improvement of inclusion efficiency, investigation of a ternary complex system is highly recommended in future studies.

**Keywords:** Febuxostat, Sulfobutylether beta-cyclodextrin, Complexation, Freeze drying, Gout

#### INTRODUCTION

Febuxostat (FBX) a non-purine, xanthine oxidase inhibitor that is commonly indicated for the treatment of chronic gout<sup>1</sup>. The chemical structure of FBX was shown in **Figure 1a** and its IUPAC name is [2-(3-cyano-4-(2methylpropoxy)-phenyl)-4-methylthiazole-5-carboxylic acid]<sup>2</sup>. According to the Biopharmaceutics

classification system (BCS), FBX is considered as a BCS class II drug that exhibits poor water solubility (0.0183 mg/ml)<sup>3</sup> and high permeability, where the dissolution rate of FBX is the rate limiting step in its absorption<sup>4</sup>. Although, the oral route for administration of FBX has shown high acceptance, it has demonstrated less oral

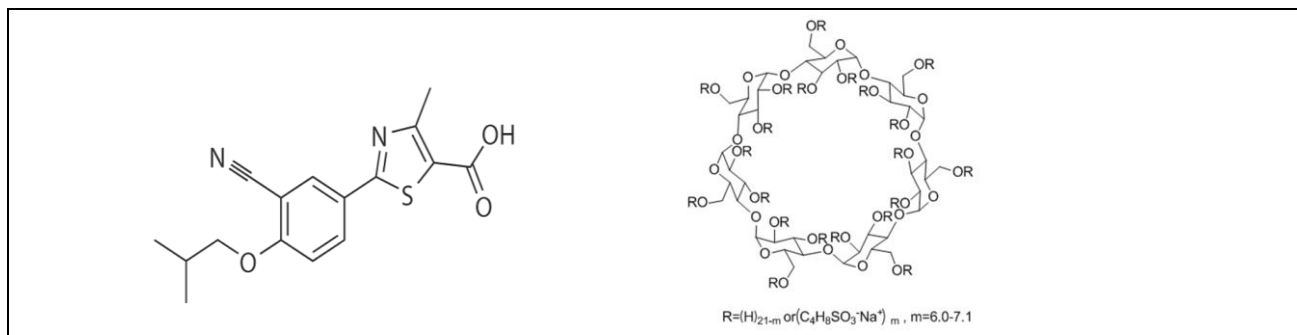


Figure 1. Chemical structure of (a) FBX and (b) SBE-βCD.

bioavailability because of its short biological half-life with significant fluctuations in plasma concentrations<sup>5</sup>. Various approaches represented by solid dispersion<sup>6</sup>, addition of cosolvents<sup>7</sup>, complexation<sup>8</sup> and size reduction<sup>9</sup> have been implemented to overcome the solubility challenges of poorly water soluble drugs. Recent studies have tried to enhance the solubility of FBX through its formulation into inclusion complexes<sup>10</sup>, nanocrystals<sup>11</sup>, and self-microemulsifying<sup>12</sup> and nanosponge drug delivery systems<sup>13</sup>.

Cyclodextrins (CDs) are cyclic oligosaccharides consisting of glucopyranose units connected by 1, 4-glycosidic linkages as shown in Figure (1b). The outer surface of CDs is hydrophilic, and the inner central cavity is hydrophobic, enabling them to form complexes with both hydrophilic and hydrophobic drug molecules<sup>14</sup>. So, it can improve the drug solubility, dissolution and bioavailability, mask the bad smell of drugs as well as reduce side effects by minimizing the dose<sup>15, 16</sup>. CDs were used in many pharmaceutical forms as micelles, vesicles, hydrogels and nanoparticles<sup>17</sup>. The natural parent β-cyclodextrin (βCD) has constrained the complexation with the hydrophobic active moieties only<sup>18</sup>. Further, modifications in the parent CDs have widened the use of modified CDs towards improving the properties of different active pharmaceutical ingredients (APIs) due to their advantages such as high efficiencies, amorphous nature<sup>19</sup>, low cost, and low toxicity<sup>20</sup>.

The modified βCD such as SBE-βCD appeared to be more water-soluble and less nephrotoxic than the unmodified βCD<sup>21</sup>. Therefore, the basis of this study was to improve the solubility of FBX using four different techniques named previously to formulate inclusion complex with SBE-βCD which as far as we know has not been studied before. Then the prepared formulations characterized by FTIR, DSC, SEM, and particle size analysis. Finally, an *in vitro* dissolution study of the inclusion complexes was conducted to verify the solubility enhancement of FBX.

## MATERIAL AND METHODS

Febuxostat (M. wt.: 316.37) was kindly donated as a gift by Eva Company for Pharmaceutical industries, Cairo, Egypt. Captisol®, Sulfbutly Ether, 7, sodium salt β-cyclodextrin (SBE-βCD, M.wt= 2163, purity 99.98%) was supplied from Cydex Inc, USA. Disodium hydrogen phosphate, Sodium dihydrogen phosphate and Methanol in analytical grade were purchased from EL-Gomhoria Company, Egypt. Distilled water was used during the studies.

### Phase solubility Study

The solubility studies for FBX were performed according to the method introduced by Higuchi and Connors<sup>22</sup>. Briefly, a known excess weight of FBX (30 mg) was added to screw capped vials containing 10 ml aqueous solution of different molar concentrations of SBE-βCD ranging from (0 to 13.5mM). These vials were allowed to be mechanically shaken in water bath shaker at 37°C±0.5. Aliquots were withdrawn from vials each 24 hours, filtered with a hydrophilic cellulose acetate sterile syringe filter (pore size 0.45 μm, diameter 25mm) and the clear filtrates were analyzed for FBX concentration using UV spectroscopy at λ<sub>max</sub> 315 nm that was obtained by scanning<sup>23</sup>. The withdrawal process was repeated every 24 hours till equilibrium was reached. Phase solubility diagram was obtained by plotting the curve between FBX solubility against SBE-βCD concentrations used. Value of stability constant (K<sub>st</sub>) was determined by using the following equation:<sup>22</sup>

$$K1:1 = \frac{St - S0}{S0(Lt - (St - S0))}$$

### Preparation of FBX inclusion complexes with SBE-βCD

Inclusion complexes of FBX were prepared in three different molar ratios (1:1, 1:3 and 1:5) by Four different methods namely physical mixture, kneading,

**Table 1. Composition of FBX/SBE-  $\beta$ CD inclusion complexes**

Preparation method	SBE- $\beta$ CD molar ratio	FBX molar ratio	Formulae code
Physical mixture	1	1	Fb1
	3		Fb2
	5		Fb3
Solvent evaporation	1	1	Fb4
	3		Fb5
	5		Fb6
Kneading	1	1	Fb7
	3		Fb8
	5		Fb9
Freeze drying	1	1	Fb10
	3		Fb11
	5		Fb12

solvent evaporation and freeze drying methods as shown in **Table (1)**. The Kneading method is the most common, low cost, and simple method used to prepare the inclusion complexes. Also, solvent evaporation method is quite simple and economic and is considered alternative to the spray drying technique<sup>24</sup>. The freeze-drying technique produces a porous, amorphous powder with a high degree of drug-CD interaction<sup>25</sup>.

#### **Physical mixture technique**

The technique relied on the idea that the selected molar ratios of FBX and SBE-  $\beta$ CD were properly blended in a ceramic mortar using a pestle for 30 minutes stirring to ensure complete homogeneity. The resulting mixtures were sieved through a sieve size (150  $\mu$ m) and subsequently stored in an airtight container for further characterization<sup>26</sup>.

#### **Kneading technique**

A specified and accurately weighed quantity of SBE-  $\beta$ CD in the selected molar ratios was added to the mortar and small quantity of water was added while triturating to get slurry like consistency. Then an accurately weighed quantity of FBX was slowly incorporated into the small parts into the slurry with continuous trituration. Trituration was continued for 1 hour. The increase in viscosity of the mixture was considered as a sign for the formation of the complex. Finally, the mixture was dried in an oven at 45°C until complete dryness. The prepared inclusion complexes were stored in an airtight container for further characterization<sup>27</sup>.

#### **Solvent evaporation technique**

This technique was achieved by dissolving equivalent weight according to selected molar ratios of the SBE-  $\beta$ CD in a glass beaker containing distilled water using hot plate magnetic stirrer till a clear solution was

obtained. The drug weight according to predecided molar ratio was added to the SBE-  $\beta$ CD solution, and then the FBX- SBE-  $\beta$ CD system was left on stirrer (24-48 hr.). The clear solutions were separated and kept at 40°C in incubator till complete evaporation of solvent and dry powder were obtained and stored in airtight container for further characterization<sup>28</sup>.

#### **Freeze drying technique**

Inclusion complexes of FBX with SBE-  $\beta$ CD in different molar ratios were prepared using freeze drying method. In this method, the specified quantity of SBE-  $\beta$ CD as calculated was transferred in a glass vial containing 10 ml of distilled water. Then the corresponding quantity of FBX was added and stirred at a hot plate magnetic stirrer for (24-48 hr.), and then clear solutions were separated. The obtained solutions were lyophilized immediately after preparation according to the following steps. The collected solutions were placed in glass vials and frozen for 24 hours at -70 °C in an ultra-cold deep freezer. Thereafter, the samples were freeze dried using a lyophilizer Christ Alpha 1-2 LD (Osterode am Harz, Germany) for 24 hrs to yield a dry powder and stored in an airtight container for further characterization<sup>29</sup>.

#### **Inclusion efficiency estimation**

The drug content in the prepared inclusion complexes was determined quantitatively by using UV spectrophotometer at 315 nm. For all the prepared inclusion complexes, accurately weighed amount of inclusion complex (30 mg) was added in 30 ml of ethanol, mixed thoroughly for 24 hr to extract the complexed FBX at ambient temperature, and then the solution was filtered by using 0.45  $\mu$ m membrane filters and measured. while this measurement providing only the amount of complexed FBX for inclusion complex prepared by freeze drying and solvent evaporation, it

provided the total FBX amount (complexed and uncomplexed) for inclusion complex prepared by kneading and physical mixture. For kneaded inclusion complex and physical mixture (30 mg) weighted precisely and washed with methanol for 20 min. and before measurement, the solutions were filtered to remove any SBE- $\beta$ CD from the solution (this providing only the amount of uncomplexed FBX)<sup>30</sup>. Appropriate dilutions were made to analyze drug content by using UV spectrophotometer (UV- 1700, Shimadzu, Japan) at 315nm. Inclusion efficiency was calculated by the following equations:<sup>31</sup>

$$\% \text{Inclusion efficiency} = (\text{Total FBX content} - \text{amount of uncomplexed FBX}) / \text{Total FBX content} * 100.$$

The suitable FBX- SBE- $\beta$ CD molar ratio for each technique was selected on the basis of inclusion efficiency determination and the selected formulations were subjected for the following characterization.

#### Characterization of inclusion complexes

The following studies were done to ensure the formation of FBX- SBE- $\beta$ CD inclusion complex on (Fb3, Fb6, Fb9, and Fb12) and to detect the best technique to prepare efficient inclusion complex.

#### Fourier Transform Infrared (IR) spectroscopy

Infrared (IR) spectra for the chosen samples were obtained at room temperature using a Shimadzu infrared spectrophotometer (FTIR Shimadzu 8400S, Lab Wrench). Samples were prepared in KBr disks (ratio 1:9) by means of a hydrostatic press. The scanning range was 400 to 4000  $\text{cm}^{-1}$ . The spectra were collected with a resolution of 4  $\text{cm}^{-1}$  using a mercury cadmium telluride (MCT) detector.

#### Differential scanning calorimetry (DSC)

The thermal behavior of the samples was examined using Shimadzu differential scanning calorimeter (DSC- 50). The measurement was carried out at according to the following conditions. The detector type was DSC-50 detector with Aluminum sealed pan cell. Sample was placed in the pan, then the temperature elevated from room temperature (20-22°C) to 300°C with temperature elevation rate 10°C/minute.

#### Particle Size and Polydispersity Index (PDI)

The selected samples were examined for particle size and polydispersity index by using a Malvern Zetasizer 300 HSA (Malvern Instruments, UK) at 25°C. The samples were dissolved in water. The dilution was performed whenever it necessary. PDI (as an indication of particle size homogeneity) was also investigated.

#### Surface morphological study

The External morphology of the selected formulae was studied by scanning electron microscopy

(JSM 6100, JEOL, Japan). The sample was mounted onto the stubs using double-sided adhesive tape and which was coated with gold palladium alloy (150–200 Å) using fine coat ion sputter.

#### In vitro dissolution studies

In vitro release studies of FBX drug and FBX - SBE- $\beta$ CD inclusion complexes prepared were carried out in distilled water, 0.1 N HCL and Phosphate Buffer pH 6.8 dissolution media using USP dissolution apparatus II (paddle method). Dissolution studies were carried out using an accurately weighted amount of selected formulae equivalent to 40 mg plain FBX in 900 ml media at 37°C $\pm$ 0.5°C at a rotation speed of 75 rpm. At preselected time intervals 5 mL samples were withdrawn, filtered immediately and replaced with 5 mL of pre-thermo stated fresh dissolution medium. Quantitative determination was performed by UV spectrophotometer at 315 nm for the releases quantity of FBX. Each measurement was performed in triplicate and graph of percent drug released versus time was plotted<sup>27</sup>.

## RESULTS AND DISCUSSION

#### Phase solubility Study

Figures 2, 3 represented the phase solubility diagram of FBX in aqueous solution of SBE- $\beta$ CD different concentrations. The solubility of FBX increased linearly with the increasing concentration of SBE- $\beta$ CD over the studied concentration range (0-10.5 mM), which could be classified as AL-type<sup>27</sup>. According to Higuchi and Connors the stoichiometric ratio of SBE- $\beta$ CD was estimated to be 1:1 as the slope of curve is less than unity (0.0251). The linear host guest correlation coefficient values obtained was  $R^2 = 0.9983$  for FBX-SBE- $\beta$ CD which was detected using linear equation of standard curve  $y = 0.0251x + 0.0411$ . The inclusion stability constant ( $K_{1:1}$ ) was calculated to be 1612.9  $\text{M}^{-1}$  suggesting the formation of a stable inclusion complex corresponding to the report that recorded drug-CD association constant ( $K_{1:1}$ ) between 200 and 5000  $\text{M}^{-1}$  is fit for improving the solubility and stability of poorly soluble drugs<sup>32</sup>. Inclusion Complexation of the drug in SBE- $\beta$ CD enhanced the solubility of the drug to a marked extent up to 5-6 folds. Thus, SBE- $\beta$ CD could significantly improve the water solubility of FBX.

#### Inclusion Efficiency estimation:

Figure 4 revealed the difference in the inclusion efficiency with the variant preparation methods. The Inclusion Efficiency (%IE) of FBX- SBE- $\beta$ CD inclusion complex at all the molar ratios was found for physical mixture ranged from (0.5 to 6%), and for

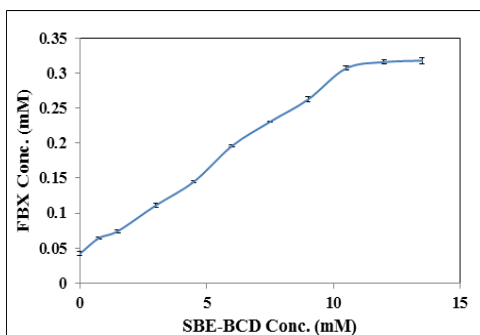


Figure 2. Phase solubility diagram for FBX-SBE-βCD (37°C).

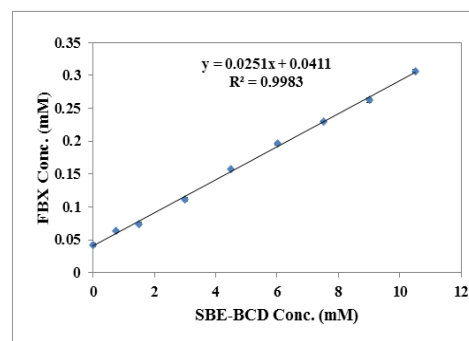


Figure 3. Phase solubility diagram for FBX/SBE-βCD (37°C).

kneaded mixture ranged from (0.86 to 18%), while the inclusion efficiency of solvent evaporation inclusion complex ranged from (1 to 25%) and for freeze dried inclusion complex ranged from (2 to 32%) according to molar ratios of (1:1 to 1:5). Results showed that all inclusion complexes prepared by various methods in molar ratio 1:5 of FBX to SBE-βCD provided higher IE% with significant difference ( $p < 0.05$ ) than those prepared in molar ratio 1:1.

#### Characterization of solid inclusion complex: Fourier Transform Infrared Spectroscopy

Infra-red is one of the tools that give reliable information about possible interactions among drug and the used excipients in the prepared formulae. This interaction can be observed through the change in positions of the main characteristic bands which are specific for certain functional groups in the compound<sup>33</sup>.

Figure (5) showed the IR spectra for FBX, SBE-βCD and different formulated inclusion complexes of the drug. The characteristic stretching peaks of FBX were  $2962.66\text{ cm}^{-1}$  and  $2873.93\text{ cm}^{-1}$  (alkane - C H group),  $2546.04\text{ cm}^{-1}$  (hydroxyl),  $2233.87\text{ cm}^{-1}$  (C≡N nitrile stretch),  $1681.93\text{ cm}^{-1}$  (C=N stretching of thiazole ring) and  $1276.88\text{ cm}^{-1}$  (ether) as shown in figure 5. FT-IR of SBE-βCD showed characteristic peaks at  $3417.86$  and  $2939.52\text{ cm}^{-1}$ , because of the O-H and C-H stretching vibrations and C-O stretching at  $1412\text{ cm}^{-1}$ . In addition, peaks at  $1651.07$ ,  $1161.15$  and  $1041.56$  corresponding to H-O-H bending of water molecules attached to CD, C-O, and C-O-C stretching of glucose units, respectively. The FTIR of physical mixture (Fb3) was established as superimposition of bands of pure drug and SBE-βCD, which indicates the obscurity of inclusion complex in this technique. Fb6 spectrum showed that most of the characteristic peaks of drug were missing (signals at  $2962.66$ ,  $2546.04$  and  $1276.88\text{ cm}^{-1}$ ) and some signals have low intensity (e.g.,  $2873.9$ ,  $2229.7$  and  $1681.93\text{ cm}^{-1}$ ), while Fb9 showed some peaks of drug were missing (signals at  $2962.66$  and  $1276.88\text{ cm}^{-1}$ ) and some

signals have low intensity (e.g.,  $2546.04$ , and  $2229.7\text{ cm}^{-1}$ ). Fb12 spectra showed peaks of drug are missing (signals at  $2962.66$ ,  $2546.04$ ,  $1681.92$  and  $1276.88\text{ cm}^{-1}$ ). Fb6 & Fb12 spectra showed more inclusion complexes formation than Fb9 as they showed more absence of most characteristic peaks of pure drug. FTIR of complexes prepared by kneading, freeze drying and solvent evaporation techniques revealed smoothing of peaks of FBX which might indicate physical interaction between FBX and SBE-βCD. The disappearance of H-O-H peak of CD in inclusion complexes could be referred to replacement of H<sub>2</sub>O molecules inside CD cavity by FBX and formation of inclusion complexes. According to literature, it could be suggested that hydrophilic portion of FBX consisting of -OH groups might have complexed with -OH in CD molecule through hydrogen bonding while hydrophobic parts in drug structure comprised of aromatic, tertiary carbon probably have made a physical interaction with C-O-C, C=C groups present in CDs. peaks were attenuated and shifted due to inclusion complex formation between drug and CDs and incorporation of lipophilic groups within CD cavity<sup>28</sup>

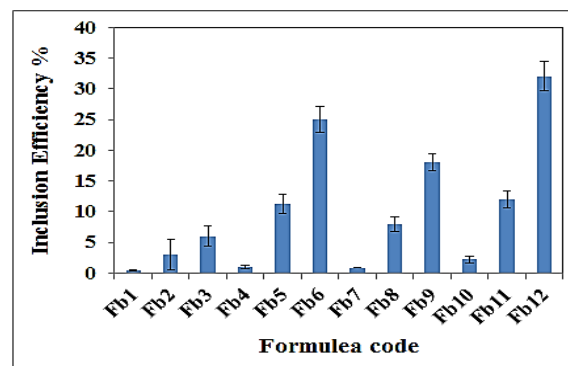


Figure 4. Inclusion efficiency % of FBX with SBE-βCD inclusion complexes.

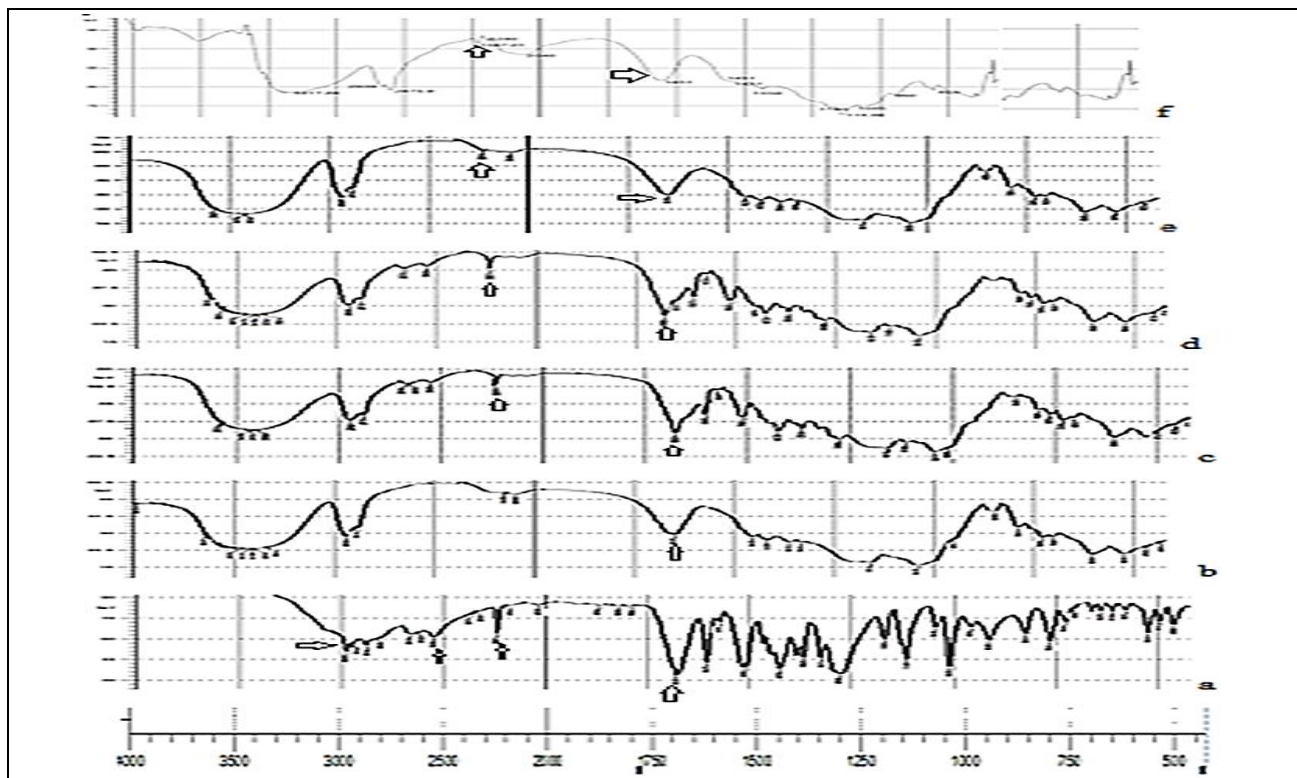


Figure 5. FTIR Spectrums of a) FBX, b) SBE-  $\beta$ CD, c) Fb3 d) Fb9, e) Fb6 and f) Fb12.

#### Differential scanning calorimetry (DSC)

Firstly, DSC was used to describe the thermal behavior of FBX either in pure or complex form. Generally, the inclusion complexation when studied with DSC describes the absence of the endothermic peak or a shift to different temperatures. The comparison between the thermograms is illustrated clearly in Figure (6). The DSC thermogram of FBX was characterized by a sharp endothermic peak at 209.3 °C, corresponding to its melting point. The SBE- $\beta$ CD exhibited a distinctive broad peak at 99.69 °C, which was identified as a water molecule loss. Thermograms of Fb3 and Fb9 revealed endothermic peaks of SBE- $\beta$ CD at 86.03 and 84.77 °C, respectively, and a low-intensity endothermic peak of the drug at 207.16 °C due to dilution factor. Fb6, and Fb12 showed a sharp fusion endothermic peak at 114.78, and 156.45 °C of CD polymer and the complete absence of a pure drug fusion peak is indicative of complete entrapment of all drug molecules in inclusion complexation with CD derivative <sup>34</sup>.

#### Particle Size and Polydispersity Index (PDI)

Particle size analysis found out of all prepared complexes to be in nano range. The particle size of pure FBX was found to be 2.7333  $\mu$ m. The mean particle size of all prepared inclusion complexes was ranged from

326.6  $\pm$  0.85 to 1272  $\pm$  0.78 nm as shown in table (2). Results revealed that the size of the nanoparticles could be related to the FBX Inclusion efficiency (IE %). These results were also in agreement with results recorded by *Abd El-Gawad, et al.* <sup>35</sup> that was showed the particle size of Econazole-HP- $\beta$ -CyD inclusion complex formed by kneading method was 269.33  $\pm$  9.02 nm with IE% of 80.83  $\pm$  3.09 %, while Econazole-HP- $\beta$ CD inclusion complex formed by freeze drying method was showed particle size 288.33  $\pm$  7.64 nm with IE % of 75.89  $\pm$  1.71 %. PDI assessing is very important as it is considered the reflection of size distribution which represents the size homogeneity between particles <sup>36</sup>. The polydispersity index was in the range of 0.353  $\pm$  0.09 to 0.776  $\pm$  0.01 for FBX- SBE- $\beta$ CD inclusion complexes. As mentioned in reports, PDI is preferred to be less than 0.5 <sup>37</sup>, so Fb12 was a good PDI of 0.353  $\pm$  0.09. The results were satisfactory for homogenous particle distribution as they did not show a significant difference ( $p > 0.05$ ) compared with PDI of 0.5.

Zeta potential is an indicator of the presence of the charge on the surface of nanoparticle, thereby indicating the degree of stability. Formulation stability is possible when the zeta potential value is nearby -30 or +30mv <sup>38</sup>. The Zeta potential for the prepared inclusion complexes was ranged from (- 14.2 to - 23.3 mV).

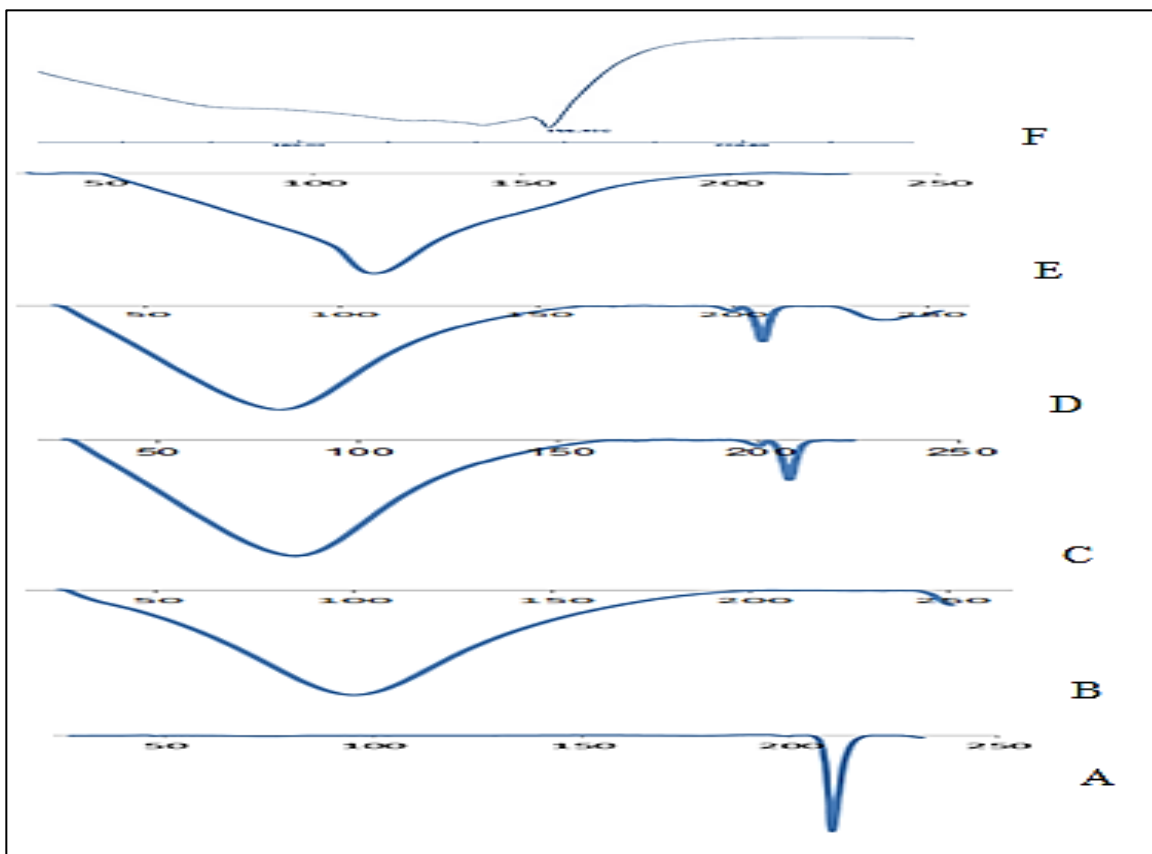


Figure 6. DSC thermogram of A) FBX, B) SBE-βCD, C) Fb3 D) Fb9, E) Fb6 and F) Fb12.

### Surface morphological study

SEM images revealed the formation of inclusion complexes for our formulae. SBE-βCD microphotographs showed hollow spherical particles with large size distribution (**Figure 7A**). While pure FBX appeared as discrete particles, rectangular needle shaped, indicating its crystalline nature (**Figure 7B**). The FBX-SBE-βCD physical mixture showed particles of SBE-βCD surrounded by FBX particles and a comparable morphology with pure components occurring separately, revealing no apparent interaction between both components in the solid state (**Figure 7C**).

On the contrary, a strong change in the original morphology and shape of both FBX and SBE-βCD particles was observed in all prepared inclusion complexes, indicating that the morphology was influenced by the selected method of preparation. The morphology of inclusion complex prepared by kneading technique (**Figure 7D**) showed the loss of sphericity, smooth surface, and reduced size of the SBE-βCD particles. FBX and SBE-βCD particles were observed to be irregularly shaped and tended to form aggregates, and it was difficult to discern between the two types of particle. This behavior could be explained by the partial

solubilization of both components during the kneading process<sup>38</sup>. The micrograph of inclusion complex prepared by solvent evaporation technique (**Figure 7E**) also revealed the formation of undifferentiated particles with a tendency to form tiny aggregates clearly different from those of the raw materials as well recorded by *Agrawal, et al, 2008*<sup>40</sup>.

Finally, the Freeze dried inclusion complex showed porous, amorphous pieces of irregular and small size with a lamellate feature (**Figure 7F**). Only the freeze drying technique allows us to obtain a real inclusion complex. This result was in full agreement with a study previously conducted by *Mazzacava et al, 2011*<sup>41</sup>

### In vitro dissolution studies

The dissolution profiles for the plain FBX, Fb3, Fb6, Fb9 and Fb12 in phosphate buffer PH 6.8, 0.1N HCl and water are presented in Figures (8, 9, and 10). It was evident from the data that Fb12 served a better dissolution profile and drug release than plain FBX over the period 120 mins in all the dissolution media. The plain FBX didn't achieve complete dissolution during

**Table 2. Percent Inclusion efficiency, particle sizes and polydispersity index and zeta potentials of the Febuoxstat / SBE-βCD inclusion complexes**

ZP (mV)	PDI	Particle size (nm)	IE. %	Formulae
-23.3±3.1	0.776± 0.01	1272 ± 0.78	6% ± 1.6	Fb3
-17±2.4	0.669± 0.02	781.3 ± 0.85	25% ± 2.1	Fb6
-18.8±3	0.655± 0.04	943.7±0.65	18% ± 1.36	Fb9
-14.2±1.8	0.353±0.09	326.6 ±0.42	32% ± 2.36	Fb12

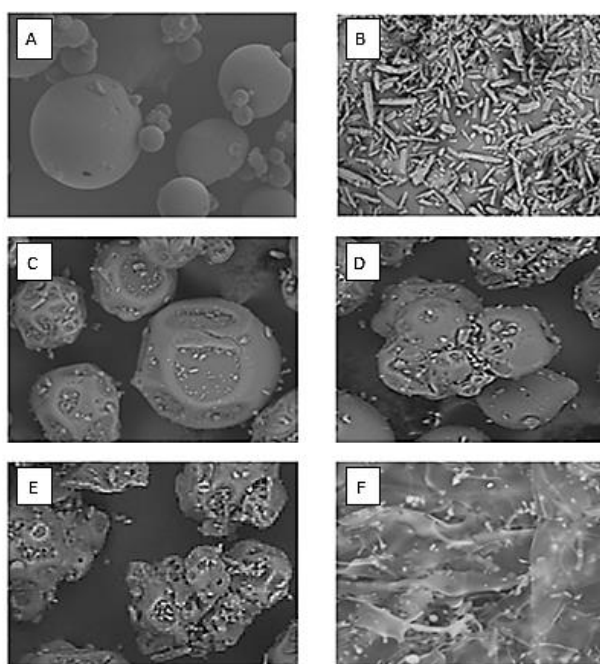


**Figure 7. Scanning electron micrographs of SBEβ-CD (A), FBX (B), Fb3 (C), Fb9 (D), Fb6 (E) and Fb12 (F).**

120 min time period and only  $7.9 \pm 1.6\%$  to  $50.8 \pm 1.3\%$  of the FBX dissolved in all the dissolution media. However, the physical mixture (Fb3) increased the dissolution of FBX  $25.6 \pm 1.52\%$  to  $56.3 \pm 1.3\%$  due to the solubilization and surfactant like effect of SBE-βCD, which improves wetting and dissolution properties of drug by reducing interfacial tension between hydrophobic drug particles and dissolution medium<sup>42</sup>.

The kneading mixture (Fb9) showed more improvement in FBX dissolution  $41.5 \pm 1.3\%$  to  $68.2 \pm 2.1\%$  than showed by physical mixture, which is in accordance with the physicochemical characterization. The improvement in dissolution of FBX is attributable to drug carrier contact and formation of stable complex caused by shear mixing, mechanical treatment, and higher wetting effect of the carrier<sup>43</sup>.

The inclusion complexes prepared by Freeze drying (Fb12) and solvent evaporation (Fb6) provided noticeable increase in FBX dissolution  $48.9 \pm 1.6\%$  to  $91.6 \pm 2.1\%$  and  $45.2 \pm 1\%$  to  $84.6 \pm 2.3\%$ , respectively. The higher dissolution rate could be attributed to disappearance of crystallinity of drug and conversion to soluble inclusion complexes that was proved above by FTIR, DSC, and SEM. In phosphate buffer PH 6.8 Fb12 showed  $91.6 \pm 1.3\%$  of FBX release after 120 minutes with a significant difference ( $p < 0.005$ ). The advantage of being amorphous provides soluble inclusion complex with higher dissolution rate as well recorded by Lankalapalli S. et al., 2018<sup>44</sup>. From the previous results freeze dried inclusion complex of FBX- SBE-βCD will be subjected to further studies to provide inclusion complex ternary system.



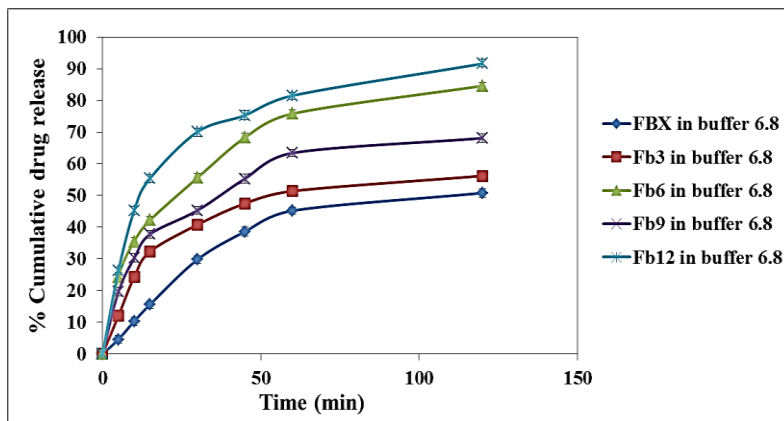


Figure 9. Graphical representation of % Cumulative drug release versus sampling time of plain FBX, Fb3, Fb6, Fb9 and Fb12 in phosphate buffer PH 6.8.

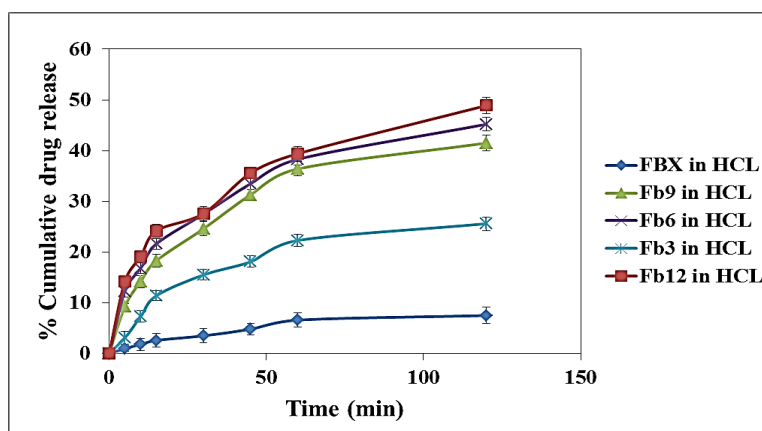


Figure 9. Graphical representation of % Cumulative drug release versus sampling time of plain FBX, Fb3, Fb6, Fb9 and Fb12 in 0.1 N HCL.

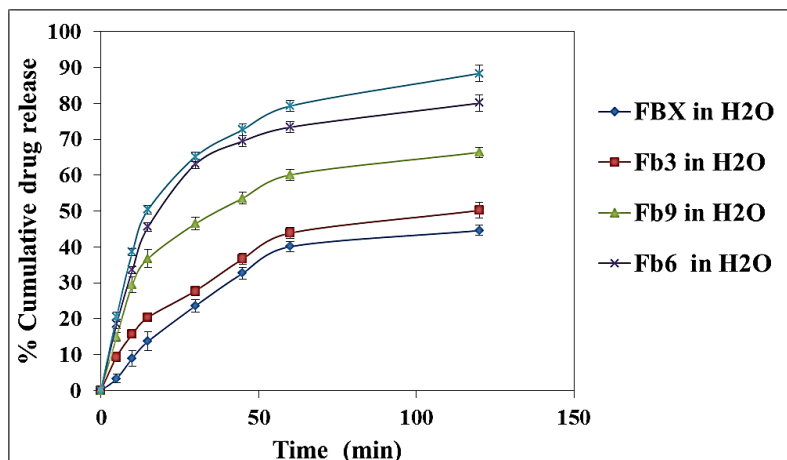


Figure 10. Graphical representation of % Cumulative drug release versus sampling time of plain FBX, Fb3, Fb6, Fb9 and Fb12 in water.

## CONCLUSION

The study has proved the significant effect of inclusion complex with sulphabutyl ether  $\beta$  Cyclodextrin on improving the dissolution of Febuxostat. Freeze drying technique showed the best inclusion efficiency of drug. The FBX-SBE- $\beta$ CD (1:5) complex showed promising results as a binary system complex which recommends it for further *in vitro* and *in vivo* study.

## Funding acknowledgement

No external funding was received.

## Conflict of interest:

The authors declare that they have no conflicts of interest regarding the publication of this paper.

## REFERENCES

1. Michael, E.; Michelle, A. Febuxostat: a selective xanthine oxidase/xanthine-dehydrogenase inhibitor for the management of hyperuricemia in adults with gout. *Clin Therap.* **2009**, 3 (1), 2503–18.
2. Paramdeep, B.; Salman, M.; Siddiqui, H. H.; Mehmood, A. A. M. T.; Singh, K. A Simple UV Spectrophotometric method for the determination of Febuxostat in bulk and pharmaceutical formulations. *IJPSR.* **2011**, 2 (10), 2655-2659.
3. Atia, N.N.; El-Gizawy, S.M.; Hosny, N.M. Facile micelleenhanced spectrofluorimetric method for picogram level determination of Febuxostat: application in tablets and in real human plasma. *Microchem. J.* **2019** doi./ 10.1016/j.microc.03.02
4. Bishoy, K.; Garry, G.; Kenneth, M.; Kevin, D.; Richard, O. Clinical pharmacokinetics and pharmacodynamics of febuxostat. *Clin Pharmacokinet.* **2017**, 5 (6), 459–75.
5. Ahuja, B.K.; Jena, S.K.; Paidi, A.; Bagri, S.; Suresh, S. Formulation, optimization and in vitro–in vivo evaluation of Febuxostat nanosuspension. *Int J Pharm.* **2015**, 478:540–552.
6. Kumar, S.; Parkash, C.; Kumar, P.; Singh, S. Application of some novel techniques for solubility enhancement of mefenamic acid, a poorly water-soluble drug. *Int. J. Pharm. Sci. Drug Res.* **2009**, 1 (3), 164-171.
7. Tang, C.; Guan, Y.X.; Yao, S.J.; Zhu, Z.Q. Solubility of Dexamethasone in Supercritical Carbon Dioxide with and without a Cosolvent. *J. Chem. Eng. Data* **2014**, 59 (11), 3359-3364.
8. Yadav, V. R.; Suresh, S.; Devi, K.; Yadav, S. Effect of cyclodextrin complexation of curcumin on its solubility and antiangiogenic and anti-inflammatory activity in rat colitis model. *AAPS PharmSciTech.* **2009**, 10 (3), 752-762.
9. Dora, C. P.; Singh, S. K.; Kumar, S.; Datusalia, A. K.; Deep, A. Development and characterization of nanoparticles of glibenclamide by solvent displacement method. *Acta Poloniae Pharmaceutica.* **2010**, 67, 283-290.
10. Kuchekar, B.S.; Divekar, V.B.; Jagdale, S.C.; Gonjari, I. Solubility enhancement and formulation of rapid disintegrating tablet of Febuxostat Cyclodextrin complex. *J. Pharm. Res.* **2013**, (1), 168–175.
11. Maddileti, D.; Jayabun, S.; Nangia, A. Soluble cocrystals of the xanthine oxidase inhibitor febuxostat. *Cryst. Growth Des.* **2013**, (13), 3188–3196.
12. Patel, P. Design and development of self microemulsifying drug delivery system of clopidogrel bisulphate. *Int. J. Pharmamedix India.* **2013**, (1), 539–553.
13. Kumar, K.K.; Srinivas, L.; Kishore, V.S.; Basha, S.N. Formulation and evaluation of poorly soluble Febuxostat Orodispersable Tablet. *Am. J. Adv. Drug Deliv.* **2014**, (2), 191–202.
14. Szejtli, J. Introduction and general overview of Cyclodextrin chemistry. *Chem Rev.* **1998**, 98, 1743–1754.
15. Brewster, M.E.; Loftsson, T. Cyclodextrins as pharmaceutical solubilizers, *Adv. Drug Deliv.* **2007**, Rev. 59, 645e666.
16. Kurkov, S.V.; Loftsson, T. Cyclodextrins. *Int. J. Pharm.* **2013**, 453, 167e180.
17. Zhang, J.X.; Ma PX. Cyclodextrin-based supramolecular systems for drug delivery: Recent progress and future perspective. *Adv Drug Deliv Rev.* **2013**, 65:1215–1233.
18. Loftson, T.; Brewster, M. Pharmaceutical applications of cyclodextrins: Drug solubilisation and stabilization. *J. Pharm. Sci.* **1996**, 85, 1017-1025.
19. Jadhav, P.; Pore, Y. Physicochemical thermodynamic and analytical studies on binary and ternary inclusion complexes of bosentan with hydroxypropyl- $\beta$ -cyclodextrin. *Bull. Fac. Pharm. Cairo Univ.* **2016**, 55, 147-154.
20. Onyeji, C.; Omoruyi, S.; Oladimeji, F. Physicochemical characterisation and dissolution properties of binary systems of pyrimethamine and 2-hydroxypropyl- $\beta$ - cyclodextrin. *Afr. J. Biotechnol.* **2009**, 8, 1651-1659.
21. Lili Ren; Jingjing Wang; Guoguang Chen. Preparation, optimization of the inclusion complex of glaucocalyxin A with sulfobutylether- $\beta$ -cyclodextrin and antitumor study. *Drug Delivery.* **2019**, doi: 10.1080/10717544.2019.1568623.
22. Higuchi, T.; Connors, K. Phase solubility techniques. *Advanced Anal. Chem. Instrumentation.* **1965**, (4), 117-212.
23. Amin, O.M.; Ammar, A.; Eladawy, S.A. Febuxostat

- loaded  $\beta$ -cyclodextrin based nanosponge tablet: an in vitro and in vivo evaluation. *J. Pharm. Investig.* **2020**, doi:10.1007/s40005-019-00464.
24. JS, P.; Kadam, D. V.; Marapur, S. C.; Kamalapur, M. V. Inclusion complex system; a novel technique to improve the solubility and bioavailability of poorly soluble drugs: a review. *Int. J. Pharm. Sci.* **2010**, 2, 29-34.
25. Cao, F.T.; Guo, J.; Ping, Q.; The Physicochemical Characteristics of Freeze-Dried Scutellarin-Cyclodextrin Tetracomponent Complexes. *Drug Dev. Ind. Pharm.* **2005**, 31, 747-56.
26. Jingjing Tang; Jiayin Bao; Xiangjun Shi; Xiaoxia Sheng ; Weike Su. Preparation, timization, and in vitro - in vivo Evaluation of Febuxostat Ternary Solid Dispersion. *J. Microencapsulation.* **2018**, doi: 10.1080/02652048.
27. Cutrignelli, A.; Lopodota, A.; Denora, N.;Iacobazzi, R. M.; Fanizza, E.; Laquintana, V.; Franco, M. A new complex of curcumin with sulfobutylether- $\beta$ -cyclodextrin: Characterization studies and in vitro evaluation of cytotoxic and antioxidant activity on HepG-2 cells. *J. Pharm. Sci* **2014**, 103 (12), 3932-3940.
28. Sadaquat, H.; Akhtar, M. Comparative effects of  $\beta$ -cyclodextrin, HP- $\beta$ -cyclodextrin and SBE7- $\beta$ -cyclodextrin on the solubility and dissolution of docetaxel via inclusion complexation. *J. Inclusion Phenomena Macrocyclic Chem.* **2020**, 96 (3), 333-351.
29. Arora, A.; Aggarwal, G.; Singh, T.G.; Singh, M.; Arora, G.; Nagpal, M. Inclusion complexes of atorvastatin calcium-sulfobutyl ether  $\beta$  cyclodextrin with enhanced hypolipidemic activity. *J. Appl. Pharm. Sci.* **2019**, (9), 60-68.
30. Santos, E.H.; Kamimura, J.A.; Hill, L.E.; Gomes, C.L. Characterization of carvacrol beta-cyclodextrin inclusion complexes as delivery systems for antibacterial and antioxidant applications. *LWT-Food Sci. Technol.* **2015**, 1, 60(1), 583-92.
31. Kuchekar, B.; Divekar, B.; Jagdale, S.; Gonjari, I. Solubility enhancement and formulation of rapid disintegrating tablet of febuxostat cyclodextrin complex. *JPR Solut.* **2013**, (1), 168-175.
32. Ruz, V.; Froeyen, M.; Busson, R.; Gonzalez, M.M.; Baudemprez, L.; Van den Mooter, G. Characterization and molecular modeling of the inclusion complexes of 2-(2-nitrovinyl) furan (G-0) with cyclodextrines. *Int. J. Pharm.* **2012**, 439, 275-285.
33. n. Pu, H.Y.; Sun, Q.M.; Tang, P.X.; Zhao, L.D.; Li, Q.; Liu, Y.Y.; Li, H. Characterization and antioxidant activity of the complexes of tertiary butylhydroquinone with betacyclodextrin and its derivatives. *Food Chem.* **2018**, 260, 183-192.
34. Li, H.; Chang, S. L.; Chang, T. R.; You, Y.; Wang, X. D.; Wang, L. W.; Zhao, B. Inclusion complexes of cannabidiol with  $\beta$ -cyclodextrin and its derivative: Physicochemical properties, water solubility, and antioxidant activity. *J. Mol. Liquids.* **2021**, 334, 116070.
35. Abd El-Gawad, A.EG.H.; Soliman, O.A.; El-Dahan, M.S. et al. Improvement of the Ocular Bioavailability of Econazole Nitrate upon Complexation with Cyclodextrins. *AAPS PharmSciTech.* **2017**, 18, 1795-1809.
36. Hadian, Z.; Maleki, M.; Abdi, K.; Atyabi, F.; Mohammadi, A.; Khaksar, R.; Preparation and Characterization of Nanoparticle  $\beta$  Cyclodextrin:Geraniol Inclusion Complexes. *Iran J Pharm Res.* **2018**, 17 (1), 39-51.
37. El-Shenawy, A.A.; Abdelhafez, W.A.; Ismail, A.; Kassem, A.A. Formulation and characterization of nanosized ethosomal formulations of antigout model drug (febuxostat) prepared by cold method: In vitro/ex vivo and in vivo assessment. *Aaps Pharmscitech.* **2020**, 21 (1):1-3.
38. Sahari, MA.; Moghimi, HR.; Hadian, Z.; Barzegar, M.; Mohammadi, A. Improved physical stability of docosahexaenoic acid and eicosapentaenoic acid encapsulated using nanoliposome containing  $\alpha$ -tocopherol. *Int. J. Food Sci. Technol.* **2016**, 51, 1075-86.
39. Fernandes, C. M.; Veiga, F. J. B. Effect of the Hydrophobic Nature of Triacetyl- $\beta$ -cyclodextrin on the Complexation with Nicardipine Hydrochloride: Physicochemical and Dissolution Properties of the Kneaded and Spray-dried Complexes. *Cham. Pharm. Bulletin.* **2002**, 50 (12), 1597-1602.
40. Agrawal, GP.; Bhargava, S. Preparation & characterization of solid inclusion complex of cefpodoxime proxetil with  $\beta$ -cyclodextrin. *Current Drug Delivery.* **2008**, 1, 5 (1), 1-6.
41. Mazzacuva, F.; Guidelli, G.; Bergonzi, M.; Bilia, A. Enhanced water solubility and stability of curcumin by microinclusion in natural and semi-synthetic cyclodextrins. *Planta Med.* **2011**, 77, PK9.
42. Aleem, O.; Kuchekar, B.; Pore, Y.; Late, S. Effect of  $\beta$ -cyclodextrin and hydroxypropyl  $\beta$ -cyclodextrin complexation on physicochemical properties and antimicrobial activity of cefdinir. *J. Pharm. Biomed. Anal.* **2008**, 47, 535-540.
43. Doiphode, D.; Gaikwad, S.; Pore, Y.; Kuchekar, B.; Late, S. Effect Of  $\beta$ -cyclodextrin complexation on physicochemical properties of zaleplon. *J. Incl. Phenom. Macrocycl. Chem.* **2008**, 62, 43-50.
44. Lankalapalli, S.; Beeraka, NMR.;Bulusu, BT. Studies on oral bioavailability enhancement of Itraconazole salts by complexation with Sulfo-butyl7 ether  $\beta$  cyclodextrin. *IJRPC.* **2018**, 8 (1), 131-43.